

# The Development of a Fast Pick-and-Place Robot with an Innovative Cylindrical Drive

Jorge Angeles

Department of Mechanical Engineering and Centre for Intelligent Machines,  
McGill University, Montreal, Quebec, Canada

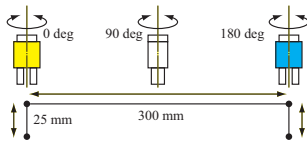
# Outline

- 1 Introduction
- 2 The C-Drive Mathematical Model
- 3 The C-Drive Prototype
- 4 The PMC Mathematical Model
- 5 The PMC Prototype
- 6 Conclusions

# Schönflies Motion Generators

## Schönflies Motion (SM)

- ▶ Three translations and one rotation about one axis of fixed direction.
- ▶ Industrial pick-and-place robots are capable of SM.
- ▶ The speed record is five test cycles per second.



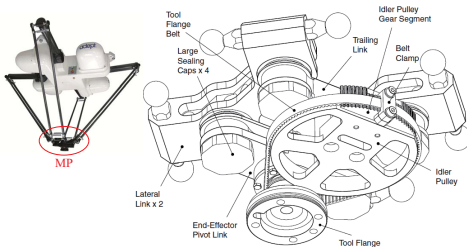
Jorge Angeles



Adept Quattro 650H

# Conventional Parallel SMG

## Adept Quattro 650H (Delta-Like Robot)



- ▶ 4 limbs
- ▶ rotation amplification required ↓
- ▶ too many extra joints to accommodate hyperstaticity ↓

# Conventional Hybrid Parallel-Serial SMG

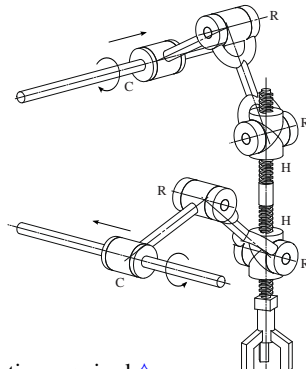
## ABB IRB 360 FlexPicker



- ▶ parallel array of 3 limbs
- ▶ telescopic Cardan shaft in series with end-effector ↓
- ▶ too many extra joints to accommodate hyperstaticity ↓

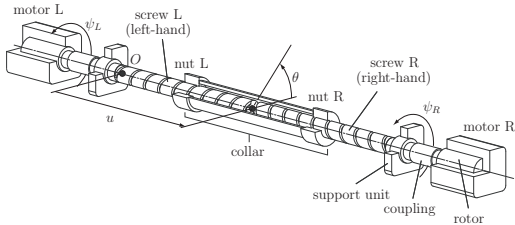
# Isostatic Schönflies Motion Generator

## CRRHHRRC Parallel PMC



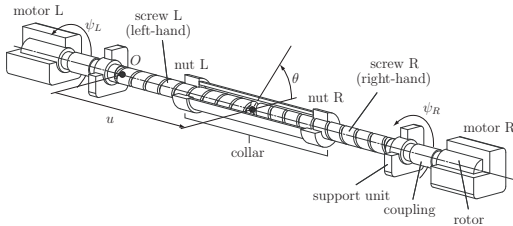
- ▶ 2 limbs
- ▶ isostatic ↑
- ▶ no rotation amplification required ↑
- ▶ proposed by C.C. Lee and P.C. Lee (2010)

# Design Principles of the C-drive



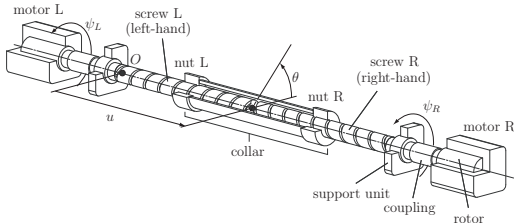
1. The number of joints must be as low as possible;
  - ▶ C joint can be synthesized by means of a serial array of two simple LKP
2. A R joint is preferred over a P joint, and a P joint over a H joint;
3. Use as many identical joints as possible, as complexity grows with their diversity

## Design Principles of the C-drive (Cont'd)



4. Reduce the diversity of the actuators; and
5. For purposes of reducing and uniformly distributing the load, fix the motors to the base

## Kinematics - Model



- ▶  $u, \theta$ : the translational and angular displacements of the C-drive collar
- ▶  $\psi_L, \psi_R$ : the angular displacements of the motors
- ▶  $p_L, p_R$  : the pitches of the left-hand screw and its right-hand counterpart

$$\frac{p_L}{2\pi}(\psi_L - \theta) = u, \quad \frac{p_R}{2\pi}(\psi_R - \theta) = u \quad (1)$$

- ▶  $p_L \neq p_R \rightarrow$  in agreement with the condition from Lie groups
- ▶ we introduce *symmetry* as the sixth design principle

$$p_L = p, \quad p_R = -p$$

# Kinematics – Jacobian

- ▶ **Dimensionally homogeneous**

Change of variable  $v \equiv (p/2\pi)\theta \rightarrow$  the actuator Jacobian  $\mathbf{J}$  is dimensionally homogeneous:

$$\mathbf{w} = \mathbf{J}\boldsymbol{\psi} \quad (3)$$

$$\mathbf{w} \equiv \begin{bmatrix} u \\ v \end{bmatrix}, \quad \mathbf{J} \equiv \frac{p}{4\pi} \begin{bmatrix} 1 & -1 \\ 1 & 1 \end{bmatrix}, \quad \boldsymbol{\psi} \equiv \begin{bmatrix} \psi_L \\ \psi_R \end{bmatrix} \quad (4)$$

- ▶ **Differential mechanism**

pure rotation: the actuators turn by the same amount in the same direction

pure translation: the actuators turn by the same amount, but in opposite directions

- ▶ **Isotropic**

$\mathbf{J}^T \mathbf{J}$  is proportional to the  $2 \times 2$  identity matrix  $\mathbf{1}$

$$\mathbf{J}^T \mathbf{J} = \frac{p^2}{8\pi^2} \mathbf{1} \quad (5)$$

- ▶ **Kinematic relation between rates**

$$\dot{\mathbf{w}} = \mathbf{J}\dot{\boldsymbol{\psi}}$$

# Dynamics

- ▶ Mathematical model describing the dynamics of the C-drive

$$\mathbf{M}\ddot{\boldsymbol{\psi}} + \mathbf{D}\dot{\boldsymbol{\psi}} + \boldsymbol{\phi}_c = \boldsymbol{\tau} \quad (7)$$

- ▶ Generalized inertia matrix  $\mathbf{M}$  ( $2 \times 2$ ):

$$\mathbf{M} \equiv \mathbf{M}_c + \mathbf{M}_h \quad (8)$$

$$\mathbf{M}_c = \mathbf{J}^T \mathbf{I}_{\text{drive}} \mathbf{J}, \quad \mathbf{I}_{\text{drive}} = \begin{bmatrix} m & 0 \\ 0 & (2\pi/p)^2 I_c \end{bmatrix}, \quad \mathbf{M}_h = I_h \mathbf{1} \quad (9)$$

$\mathbf{M}_c$ : generalized inertia matrix of the collar

$\mathbf{M}_h$ : generalized inertia matrix of the screws of the ballscrews

$I_c, I_h$ : collar and screws moment of inertia about C-drive axis

# Dynamics: Friction

- ▶ Mathematical model describing the dynamics of the C-drive

$$\mathbf{M}\ddot{\boldsymbol{\psi}} + \mathbf{D}\dot{\boldsymbol{\psi}} + \boldsymbol{\phi}_c = \boldsymbol{\tau} \quad (10)$$

- ▶ Viscous and Coulomb friction forces:

$$\mathbf{D} \equiv \begin{bmatrix} \beta + \frac{1}{2}\gamma & -\frac{1}{2}\gamma \\ -\frac{1}{2}\gamma & \beta + \frac{1}{2}\gamma \end{bmatrix}, \quad \boldsymbol{\phi}_c = \begin{bmatrix} \delta \text{sgn}(\dot{\psi}_L) + \eta \text{sgn}(\dot{\psi}_L - \dot{\psi}_R) \\ \delta \text{sgn}(\dot{\psi}_R) + \eta \text{sgn}(\dot{\psi}_R - \dot{\psi}_L) \end{bmatrix} \quad (11)$$

$\beta, \gamma$ : viscous friction coefficients

$\delta, \eta$ : Coulomb friction coefficients

# State-Space Representations

## Standard Linear State-Space Form

$$\dot{\mathbf{x}} = \mathbf{Ax} + \mathbf{Bu} \quad (12)$$

$$\mathbf{y} = \mathbf{Cx} \quad (13)$$

with the output vector  $\mathbf{y}$  defined as

$$\mathbf{y} \equiv \boldsymbol{\psi} \quad (14)$$

$\boldsymbol{\psi}$ : vector of joint (motor) displacements

$\mathbf{x}$ : state vector

$\mathbf{u}$ : input vector, i.e., applied motor torques

In the following models, the state vectors are dimensionally homogeneous

## State-Space Representations: Collar Coordinates as States

- ▶ Second-order generalized-coordinate model:

$$\mathbf{M}\ddot{\boldsymbol{\psi}} + \mathbf{D}\dot{\boldsymbol{\psi}} + \boldsymbol{\phi}_c = \boldsymbol{\tau} \quad (15)$$

- ▶ Substituting  $\boldsymbol{\psi}$  with its expression in terms of collar coordinates  $\mathbf{w}$ :

$$\mathbf{M}\mathbf{J}^{-1}\ddot{\mathbf{w}} + \mathbf{D}\mathbf{J}^{-1}\dot{\mathbf{w}} = \boldsymbol{\tau} \quad (16)$$

- ▶ Upon premultiplication by Jacobian matrix  $\mathbf{J}$ :

$$\underbrace{\mathbf{J}\mathbf{M}\mathbf{J}^{-1}}_{\mathbf{E}}\ddot{\mathbf{w}} + \underbrace{\mathbf{J}\mathbf{D}\mathbf{J}^{-1}}_{\mathbf{G}}\dot{\mathbf{w}} = \mathbf{J}\boldsymbol{\tau} \quad (17a)$$

$$\mathbf{E} \equiv \begin{bmatrix} v_2^2 & 0 \\ 0 & v_1^2 \end{bmatrix}, \quad \mathbf{G} \equiv \begin{bmatrix} \delta_2 & 0 \\ 0 & \delta_1 \end{bmatrix}, \quad i = 1, 2 \quad (17b)$$

- ▶  $v_i^2$  and  $\delta_i$  are the eigenvalues of  $\mathbf{M}$  and  $\mathbf{D}$ , respectively

## Dynamics in Monic Form

- The dynamics is obtained in *monic* form, with Coulomb friction forces neglected

$$\ddot{\boldsymbol{\sigma}} + \Theta \dot{\boldsymbol{\sigma}} = \mathbf{u} \quad (18)$$

via the substitutions

$$\Theta \equiv \sqrt{\mathbf{E}}^{-1} \mathbf{G} \sqrt{\mathbf{E}}^{-1}, \quad \boldsymbol{\sigma} \equiv \sqrt{\mathbf{E}} \mathbf{w}, \quad \mathbf{u} \equiv \sqrt{\mathbf{E}}^{-1} \mathbf{J} \boldsymbol{\tau} \quad (19)$$

where

$$\Theta \equiv \begin{bmatrix} \vartheta_2 & 0 \\ 0 & \vartheta_1 \end{bmatrix}, \quad \sqrt{\mathbf{E}}^{-1} \mathbf{J} \equiv \frac{p}{4\pi} \begin{bmatrix} 1/\nu_2 & -1/\nu_2 \\ 1/\nu_1 & 1/\nu_1 \end{bmatrix} \quad (20)$$

with

$$\vartheta_i \equiv \delta_i / \nu_i^2, \quad i = 1, 2 \quad (21)$$

## State-Space Representations: 2D and 4D

$$\dot{\mathbf{x}} = \mathbf{Ax} + \mathbf{Bu}, \quad \mathbf{y} = \mathbf{Cx} \quad (22)$$

### 2D Representation

$$\mathbf{x} \equiv \dot{\boldsymbol{\sigma}} \quad (23a)$$

$$\mathbf{y} \equiv \psi \quad (23b)$$

$$\mathbf{A} \equiv -\Theta, \quad \mathbf{B} \equiv \mathbf{1} \quad (23c)$$

$$\mathbf{C} \equiv \mathbf{J}^{-1} \sqrt{\mathbf{E}}^{-1} \quad (23d)$$

### 4D Representation

$$\mathbf{x} \equiv \begin{bmatrix} \boldsymbol{\sigma}^T & \dot{\boldsymbol{\sigma}}^T \Theta^{-T} \end{bmatrix}^T \quad (24a)$$

$$\mathbf{y} \equiv \psi \quad (24b)$$

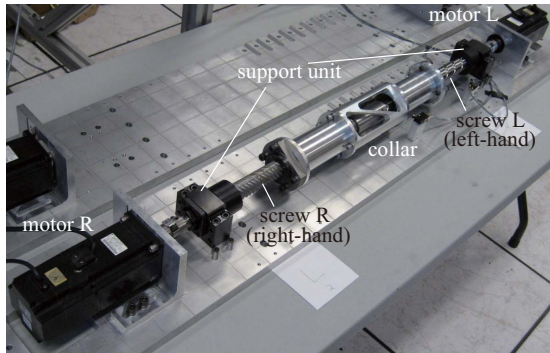
$$\mathbf{A} \equiv \begin{bmatrix} \mathbf{0} & \Theta \\ \mathbf{0} & -\Theta \end{bmatrix}, \quad \mathbf{B} \equiv \begin{bmatrix} \mathbf{0} \\ \Theta^{-1} \end{bmatrix} \quad (24c)$$

$$\mathbf{C} \equiv \begin{bmatrix} \mathbf{J}^{-1} \sqrt{\mathbf{E}}^{-1} & \mathbf{0} \end{bmatrix} \quad (24d)$$

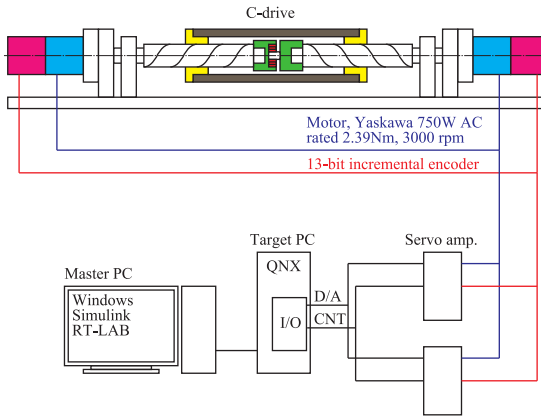
- ▶ **1** and **0** are the  $2 \times 2$  identity and zero matrices, respectively
- ▶ The 2D system is simpler; the response of the system is readily derived
- ▶ The 4D system has an observable state vector, as  $\psi$  is measured



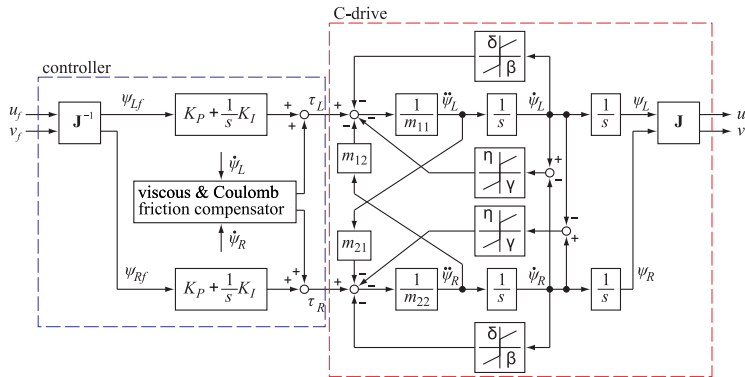
# Mechanism



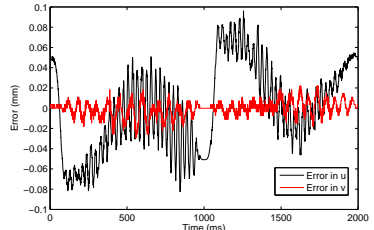
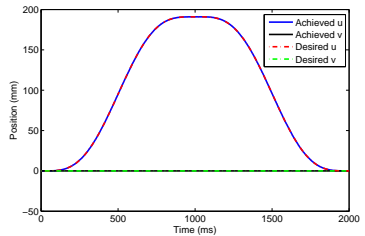
# Control System



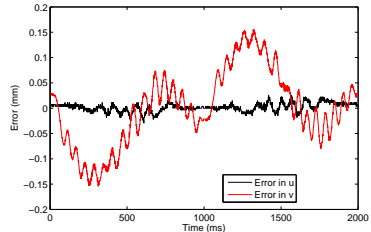
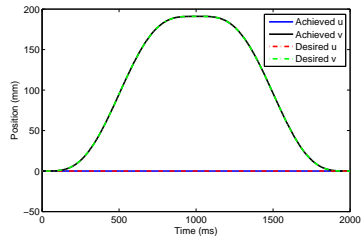
# Control Architecture



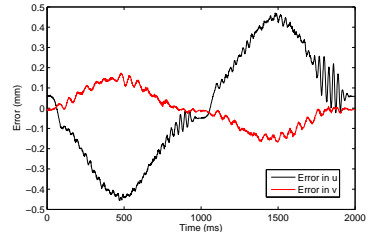
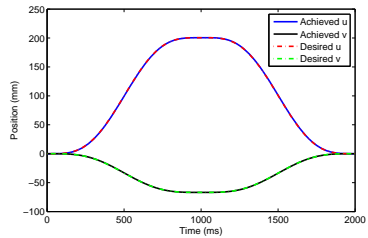
# Pure Translation



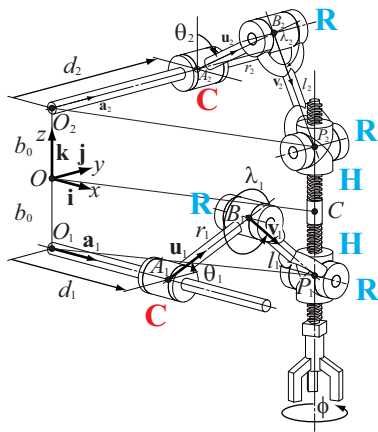
# Pure Rotation



# Helical Motion



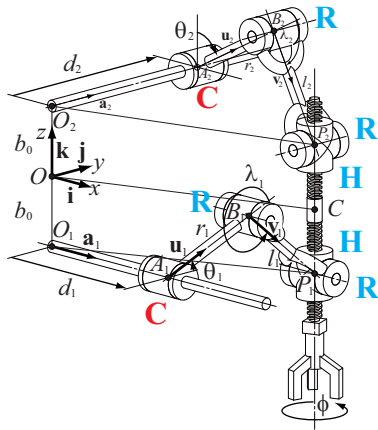
# Kinematic Model of the PMC



- ▶ The PepperMill-Carrier (PMC): CRRHHRRC parallel mechanism
- ▶  $d_i$  and  $\theta_i$  (for  $i = 1, 2$ ): the translational and rotational displacement variables of the  $i$ th C joint
- ▶ The pose  $\mathbf{x}$  of the PepperMill is given by  $\mathbf{c} = [x, y, z]^T$ , the position vector of point  $C$ , and angle  $\phi$ :

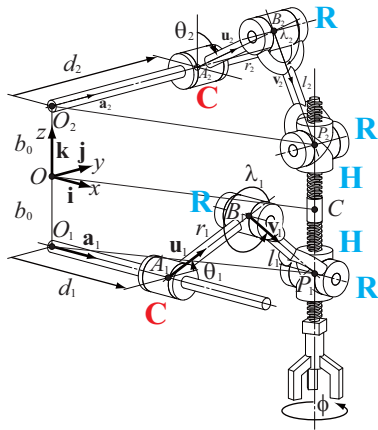
$$\mathbf{x} \equiv \begin{bmatrix} \mathbf{c} \\ \phi \end{bmatrix} \quad (25)$$

# Kinematic Model of the PMC



- ▶ Points  $O_i$ : the intersection of the  $i$ th-drive axis with the common normal to the two, for  $i = 1, 2$
- ▶ The fixed origin  $O$  of the base frame is set at the midpoint of segment  $\overline{O_1O_2}$
- ▶  $\mathbf{i}, \mathbf{j}$  and  $\mathbf{k}$ : unit vectors parallel to the  $x$ ,  $y$  and  $z$  axes

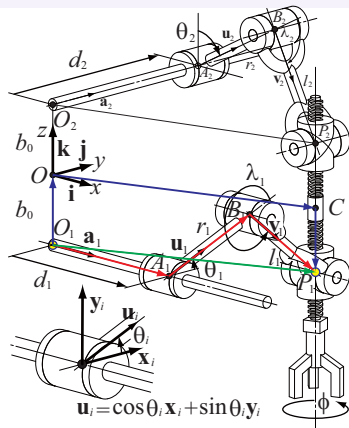
# Kinematic Model of the PMC



For  $i = 1, 2$ ,

- ▶  $\lambda_i$ : the angle of rotation of the proximal passive R joint
- ▶  $\mathbf{u}_i$  and  $\mathbf{v}_i$ : unit vectors parallel to the axes of the proximal and the distal links
- ▶  $r_i$  and  $l_i$ : the lengths of the proximal and the distal links
- ▶ The end of the distal link of the  $i$ th limb is coupled with the passive R pair of the PepperMill at point  $P_i$

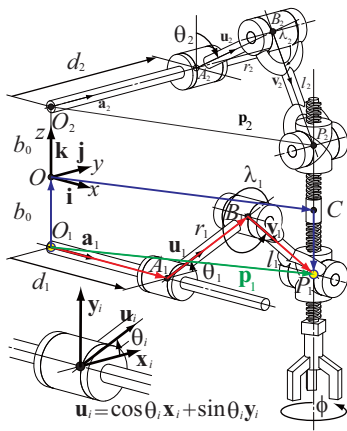
## PMC Inverse Displacement Analysis



- ▶ Displacement analysis performed via loop-closure equations
- ▶ The translational displacements of each C-drive are obtained directly from the horizontal displacements of the PepperMill:

$$d_1 = x, \quad d_2 = y \quad (26)$$

# PMC Inverse Displacement Analysis



- The angular displacements  $\theta_i$ ,  $i = 1, 2$ , of each C-drive are computed from

$$(\mathbf{q}_i^T \mathbf{x}_i) \cos \theta_i + (\mathbf{q}_i^T \mathbf{y}_i) \sin \theta_i \quad (27)$$

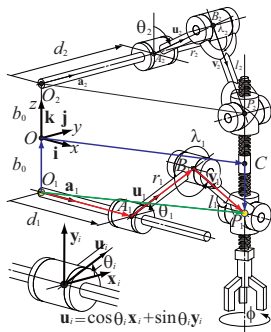
$$= \frac{\mathbf{q}_i^T \mathbf{q}_i + r_i^2 - l_i^2}{2r_i}$$

where

$$\mathbf{q}_i \equiv \mathbf{p}_i - d_i \mathbf{a}_i \quad (28)$$

# Forward Displacement Analysis

## CRRHHRRC Parallel PMC



- ▶ The horizontal displacements of the PepperMill are simply

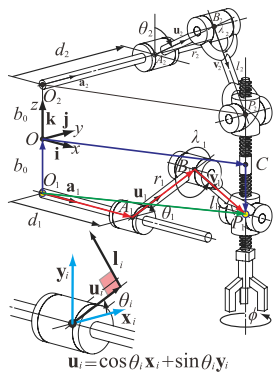
$$x = d_1, \quad y = d_2 \quad (29)$$

- ▶ The vertical and angular displacements of the PepperMill are computed from

$$\begin{bmatrix} 1 & p_1 \\ 1 & p_2 \end{bmatrix} \begin{bmatrix} z \\ \phi \end{bmatrix} = \begin{bmatrix} r_1 \sin \theta_1 + l_1 \sin(\theta_1 + \lambda_1) - b_0 \\ r_2 \cos \theta_2 + l_2 \cos(\theta_2 + \lambda_2) + b_0 \end{bmatrix} \quad (30)$$

- ▶ The leftmost matrix is invertible when  $p_1 \neq p_2$

# PMC Kinematics: Jacobian Analysis



- The PepperMill pose  $\mathbf{x}$  and proximal link displacements  $\boldsymbol{\theta}$  are

$$\mathbf{x} \equiv [x \quad y \quad z \quad \phi]^T \quad (31)$$

$$\boldsymbol{\theta} \equiv [d_1 \quad d_2 \quad \theta_1 \quad \theta_2]^T \quad (32)$$

- Vectors  $\mathbf{l}_i$  are defined as shown in the figure, for  $i = 1, 2$

# PMC Kinematics: Jacobian Analysis

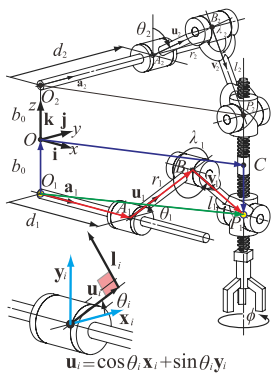
► Kinematics relation

$$\mathbf{A}\dot{\mathbf{x}} = \mathbf{B}\dot{\boldsymbol{\theta}} \quad (33)$$

where Jacobian matrices  $\mathbf{A}$  and  $\mathbf{B}$  are

$$\mathbf{A} = \begin{bmatrix} 1 & 0 & 0 & 0 \\ 0 & 1 & 0 & 0 \\ 0 & v_1^y & v_1^z & p_1 v_1^z \\ v_2^x & 0 & v_2^z & p_2 v_2^z \end{bmatrix} \quad (34)$$

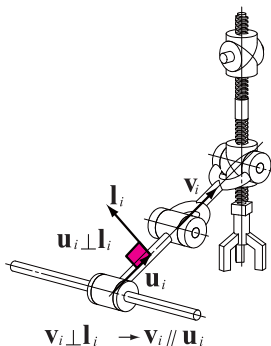
$$\mathbf{B} = \begin{bmatrix} 1 & 0 & 0 & 0 \\ 0 & 1 & 0 & 0 \\ 0 & 0 & \mathbf{v}_1^T \mathbf{l}_1 & 0 \\ 0 & 0 & 0 & \mathbf{v}_2^T \mathbf{l}_2 \end{bmatrix} \quad (35)$$



$$\mathbf{u}_i = \cos\theta_i \mathbf{x}_i + \sin\theta_i \mathbf{y}_i$$

For  $i = 1, 2$  and  $j = x, y, z$ ,  $v_i^j$  is the  $j$ th component of  $\mathbf{v}_i$

# The Singularity of the First Kind (inverse-kinematics singularity)



$$\mathbf{B} = \begin{bmatrix} 1 & 0 & 0 \\ 0 & 1 & 0 \\ 0 & 0 & \mathbf{v}_1^T \mathbf{l}_1 \\ 0 & 0 & \mathbf{v}_2^T \mathbf{l}_2 \end{bmatrix}$$

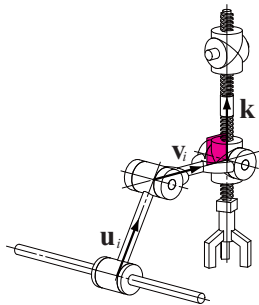
- The singularity of the first kind occurs when the Jacobian matrix  $\mathbf{B}$  is singular, i.e., when

$$\det(\mathbf{B}) \equiv (\mathbf{v}_1^T \mathbf{l}_1)(\mathbf{v}_2^T \mathbf{l}_2) = 0 \quad (36)$$

- Geometrically, this singularity occurs when  $\mathbf{v}_1 \perp \mathbf{l}_1$  or  $\mathbf{v}_2 \perp \mathbf{l}_2$ , i.e., when the unit vector  $\mathbf{u}_i$  of the proximal link and the unit vector  $\mathbf{v}_i$  of the distal link are parallel in at least one limb

# The Singularity of the Second Kind (direct-kinematics singularity)

- The singularity of the second kind occurs when the Jacobian matrix  $\mathbf{A}$  is singular:



$$\mathbf{v}_i = \begin{bmatrix} v_i^x \\ v_i^y \\ v_i^z \end{bmatrix}$$

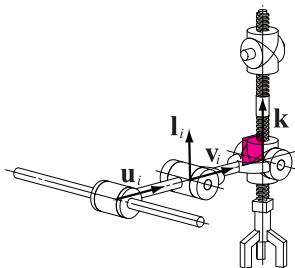
$$\begin{aligned} \det(\mathbf{A}) &= \det \left( \begin{array}{cc|cc} 1 & 0 & 0 & 0 \\ 0 & 1 & 0 & 0 \\ \hline 0 & v_1^y & v_1^z & p_1 v_1^z \\ v_2^x & 0 & v_2^z & p_2 v_2^z \end{array} \right) \\ &= \det \begin{pmatrix} 1 & 0 \\ 0 & 1 \end{pmatrix} \det \begin{pmatrix} v_1^z & p_1 v_1^z \\ v_2^z & p_2 v_2^z \end{pmatrix} \\ &= v_1^z v_2^z (p_2 - p_1) = 0 \end{aligned} \quad (37)$$

- The pitches of the two H joints of the PepperMill are distinct:

$$p_1 \neq p_2 \quad (38)$$

- Geometrically, these conditions occur when the unit vector of the distal link of at least one limb is normal to the  $z$ -axis

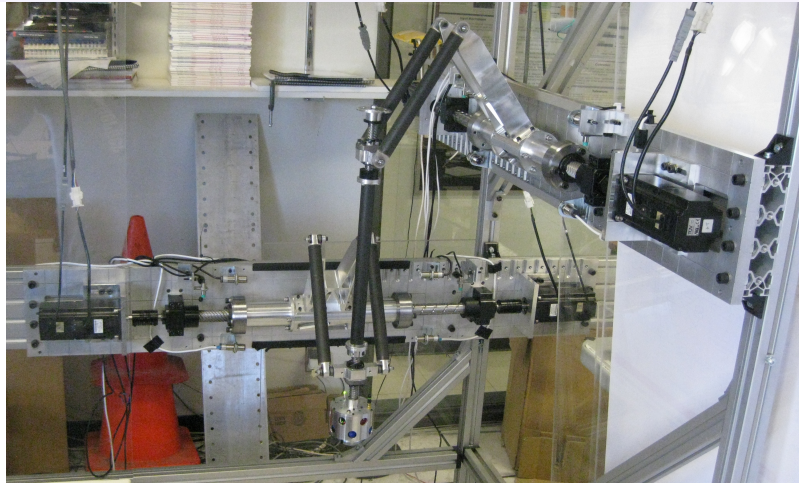
# The Singularity of the Third Kind (complex-kinematics singularity)



- ▶ The singularity of the third kind occurs when the the two Jacobian matrices **A** and **B** become singular
  
$$\det(\mathbf{A}) = v_1^z v_2^z (p_2 - p_1) = 0$$
$$\det(\mathbf{B}) = (\mathbf{v}_1^T \mathbf{l}_1)(\mathbf{v}_2^T \mathbf{l}_2) = 0$$
  
- ▶ This singularity depends on the robot architecture. Given the symmetries with which the PepperMill was designed, this robot admits the singularity of the third kind, as illustrated in the figure

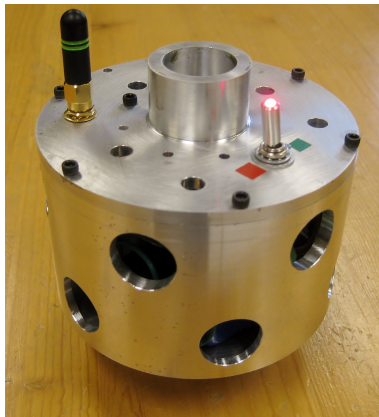
# PepperMill Motion

## PMC Prototype



# Magnetic Gripper Functionality

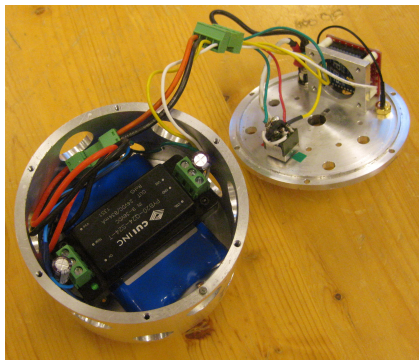
## Wireless Magnetic Gripper Assembly



- ▶ 10W 24VDC electromagnet actuated wirelessly
- ▶ Lithium-Ion battery recharged in circuit
- ▶ 1 mW Xbee radio communicates via 2.4 GHz 802.15.4 protocol
- ▶ Digital I/O line passing between control module and embedded module

# Magnetic Gripper Features

## Wireless Magnetic Gripper Assembly



- ▶ External 1/4 wave monopole antenna
- ▶ Uses gripper enclosure as ground plane
- ▶ Robust 802.15.4 protocol supports point-to-point, point-to-multipoint and peer-to-peer network topologies
  - ▶ Scalable: multiple modules may be used in close proximity
  - ▶ Can be configured to actuate different types of gripper (e.g. clamp)

# Mechanical Interference Detection

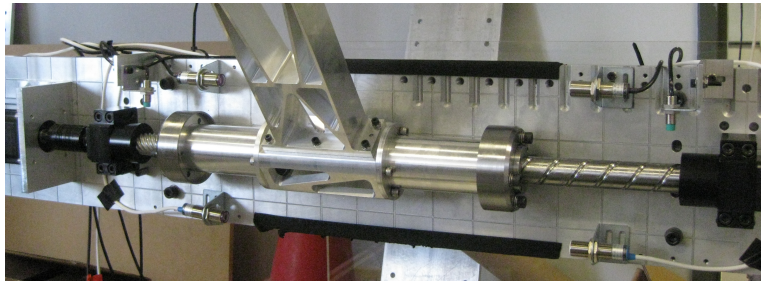
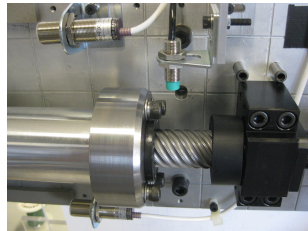


Figure: Single C-drive

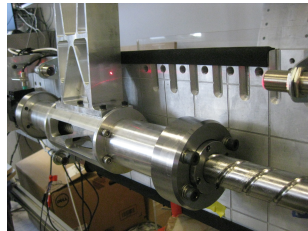
- ▶ Robot dimensions chosen such that moving links cannot collide
- ▶ Proximal links—the C-drives—can collide with the base in four ways
- ▶ C-drives present unusual challenges in detecting extreme positions

# Mechanical Interference Detection Switches: Contactless

## Translation Limit Switch



## Rotation Limit Switch



- ▶ Magnetic proximity switch detects edge of C-drive cap
- ▶ Cap edge angled 30° to increase sensor sensitivity

- ▶ Laser photo-electric switch
- ▶ Laser beam interrupted by proximal link when close to extreme position

# Conclusions

- ▶ The development of an innovative two-DOF cylindrical drive was described
- ▶ The kinematics and dynamics of the C-drive were derived, as well as convenient state-space representations thereof
- ▶ The C-drive mechanism and control system were described; test results yielded low error
- ▶ PMC prototype assembly shown, including safety features
- ▶ The singularity analysis of the PMC was reported
- ▶ The embedded electromagnetic gripper was described

## Acknowledgements

The work described here is the result of team work. Team members: Damien Trézieres, Master's Visitor from Lyon, France; Takashi Harada, Kinki U., Japan; Thomas Friedlaender, M.Eng. student at McGill U.

The support from various sources is to be acknowledged: NSERC (Canada's Natural Sciences and Engineering Research Council), James McGill Professorship to J. Angeles; Japan's MEXT-supported Program for the Strategic Research Foundation to Private Universities; and THK Co., Ltd for their support.